Solar Physics
DOI: 10.1007/•••••-•••-•••-••••-•

Sub-terahertz, microwaves and high energy emissions during the December 6, 2006 flare, ∼ 18:40 UT

Pierre Kaufmann[1,2] · **Gérard Trottet**[3] · **C. Guillermo Giménez de Castro**[1] · **Jean-Pierre Raulin**[1] · **Säm Krucker**[4] · **Albert Y. Shih**[4] · **Hugo Levato**[5]

Abstract The presence of a solar burst spectral component with flux density increasing with frequency in the sub-terahertz range, spectrally separated from the well-known microwave spectral component, bring new possibilities to explore the flaring physical processes, both observational and theoretical. The solar event of December 6, 2006, starting at about 18:30 UT, exhibited a particularly well-defined double spectral structure, with the sub-THz spectral component detected at 212 and 405 GHz by SST and microwaves (1-18 GHz) observed by OVSA. Emissions obtained by instruments in satellites are discussed with emphasis to TRACE UV, GOES soft X-rays and RHESSI X- and γ-rays. The sub-THz impulsive component had its closer temporal counterpart only in the higher energy X- and γ-rays ranges. The spatial positions of the centers of emission at 212 GHz for the first flux enhancement were clearly displaced by more than one arc-minute from positions at the following phases. The observed sub-THz fluxes and burst source plasma parameters were found difficult to be reconciled to a purely thermal emission component. We discuss possible mechanisms to explain the double spectral components at microwaves and in the THz ranges.

1. Introduction

Although the nature of the particle acceleration mechanisms in solar flares is not **fully** understood, their by-products are usually well described and studied. The presence of an independent flare terahertz spectral emission component,

[1] Centro de Rádio-Astronomia e Astrofísica Mackenzie, Escola de Engenharia, Universidade Presbiteriana Mackenzie, Rua Consolação 896, 01302-907 São Paulo, SP, Brazil. email:kaufmann@craam.mackenzie.br
[2] Centro de Componentes Semicondutores,Universidade Estadual de Campinas, Campinas, SP, Brazil.
[3] LESIA, Observatoire de Paris-Meudon, Meudon, France.
[4] Space Sciences Laboratory, University of California Berkeley, Berkeley, CA, USA.
[5] Complejo Astronómico El Leoncito, San Juan, Argentina.

simultaneously to the well known component at microwaves, brought new challenges and possibly new clues to explain the nature of the flare primary accelerator (Kaufmann *et al.*, 2004). The vast majority of microwave bursts exhibits typical spectra with maximum fluxes in the range 5-20 GHz. Fewer observations carried out at higher frequencies, up to 100 GHz, have shown uncommon events exhibiting fluxes increasing with frequency, some showing complex spectral shapes, and inflections somewhere between 30-70 GHz, and other flattening at higher frequencies (Croom, 1970; Croom, 1971b; Shimabukuro, 1970; Cogdell, 1972; Akabane *et al.*, 1973; Kaufmann *et al.*, 1985; Ramaty *et al.*, 1994; Bastian, Fleishman, and Gary, 2007; Altyntsev *et al.*, 2008). The newly discovered emission intensity increases with frequency at sub-THz frequencies as a new spectral component clearly separated from the well known emission spectrum at microwaves, displaying a double-structure in the microwave - submillimeter range of wavelengths.

We will describe and discuss the solar flare of December 6, 2006, starting at about 18:30 UT that exhibited a distinct THz spectral component throughout the event duration as observed by the solar submillimeter telescope (SST) at 212 and 405 GHz (Kaufmann *et al.*, 2007) until 18:55 UT. Minutes later, the OVSA **(Owens Valley Solar Array)** has detected the largest decimeter narrow band spikes ever observed (Gary, 2008). SST observations were compared to decimeter to microwaves obtained by the Owens Valley Solar Array and to X- to γ-rays detected by RHESSI satellite. These observations were complemented by TRACE satellite UV movies. The event corresponds to a 3B flare on AR 0930, S06E63, starting at 18:32 UT, maximum at 18:45 UT, and at 21:35 UT, with soft X-ray GOES class X6.5.

2. Multiple wavelength time profiles and spectra

We show in Figure 1 the burst intensity time profiles at two microwave frequencies, submillimeter-waves, soft, hard X-rays and γ-rays. Despite of good clear-sky conditions at SST El Leoncito site the atmosphere measured attenuation was high. It was measured at 15:30 UT, before the burst, providing optical depths τ of 0.35 and 2.6 nepers at 212 and 405 GHz, respectively. At a mean elevation angle of 55° the correction factors to correct antenna noise temperatures were of 1.5 and 24 respectively. There were indications of transmission changes after 18:55 UT when the 405 GHz data corrections became inconsistent. Since there were no other atmosphere transmission measurements, the analysis was interrupted. Small changes in large values of τ, as was the case for 405 GHz, may bring significant changes in correction factors, which cannot be taken into account here. The labels at the top of Figure 1 refer to: the precursor-like first enhancement **(A)**, the maximum impulsive-like phase **(B)** and following time structures **(C)**. In phase **(B)** the sub-THz time profile **compares to the bulk of impulsive emissions at microwaves, $>$ 2.7 MeV gamma-rays and to a lesser extent to $>$ 85 keV hard X-rays**.

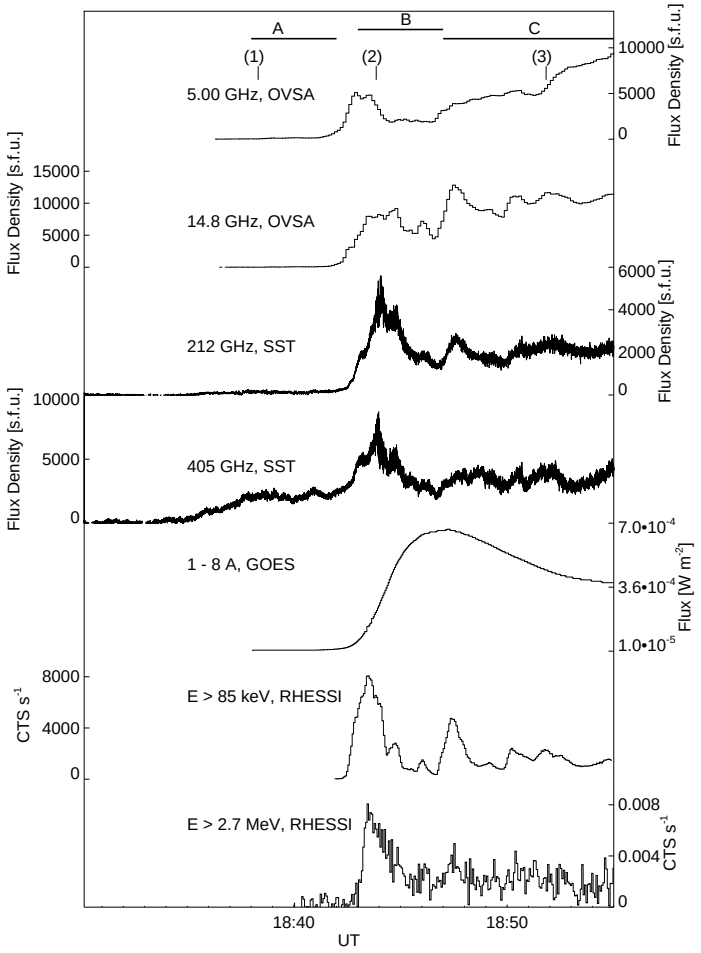

Figure 1. Time profiles for the December 6, 2006 solar burst. From top to bottom: two microwaves from OVSA; the two SST frequencies; GOES soft X-rays; RHESSI at hard X-rays and at γ-rays. Labels **(A)**, **(B)** and **(C)** are the time intervals for which the positions were taken for the 212 GHz burst centroids of emission, shown in Figure 4. Labels 1, 2 and 3 are the times when the burst sub-THz and microwave spectra were taken, shown in Figure 2.

Examples for the 212 and 405 GHz spectra are shown in Figure 2 sampled over 8.1 seconds averages (to be comparable to the OVSA time resolution) on the times labeled 1-3 at the top of Figure 1. The burst spectra exhibited the two distinct components throughout the whole event duration, one peaking at microwaves, as derived from Owens Valley Solar Array, and another sub-THz component increasing with frequency, as observed by the SST. The uncertainty bars **indicate the extreme limits set empirically for** a conservative assumption of 10% changes in the optical depths. The sub-THz spectral component together with the independent microwave component is strikingly evident at the precursor-like phase **(A)**, being present at the impulsive phase **(B)**, and suggested

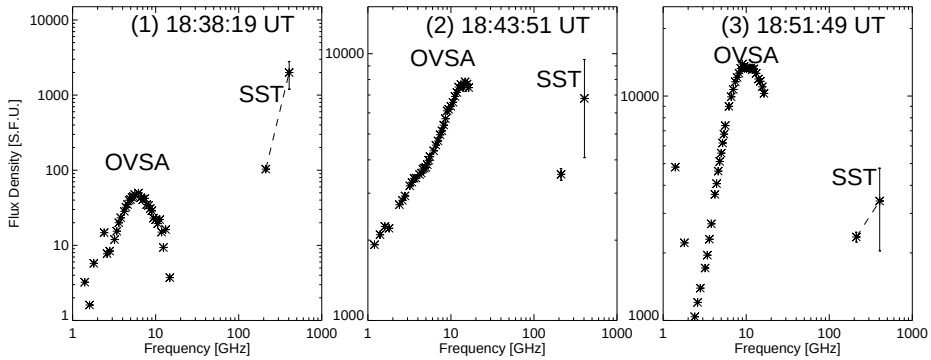

Figure 2. Complete burst spectra, from decimeter to submillimeter waves, for the burst times 1-3 labeled at the top of Figure 1. Bars refer to an arbitrary **uncertainty** assumption of 10% changes in the optical depths. The presence of the sub-THz component is particularly well defined for the precursor-like structure, the impulsive phase, and suggested for the following phase.

for the following phase **(C)**. **The OVSA microwave spectra for the three phases are shown in Figure 2. They are usually attributed to gyrosynchrotron emission by mildly relativistic electrons** (Dulk, 1985)**. The maximum emission turnover frequencies change with time, as it has been known for other bursts** (Croom, 1971a**;** Roy, 1979**;** Nita, Gary, and Lee, 2004)**. Figure 3 shows the time variation of microwave turnover frequencies f_s (which in some cases cannot be unambiguously determined because apparently it exceeded the maximum OVSA limit), the GHz spectral index for $f > f_s$, the GHz flux at f_s and the sub-THz spectral index. The uncertainty bar indicates the extreme limits set empirically for a conservative assumption of 10% changes in the optical depths**. Rapid superimposed time structures **were present at both sub-THz frequencies and** will be discussed in a separate paper.

3. Positions, sizes and fluxes

The positions of burst centers of emission can be determined at 212 GHz by comparing the relative intensities (corrected antenna temperatures) of the SST three partially overlapping beams (Georges *et al.*, 1989; Costa *et al.*, 1995; Giménez de Castro *et al.*, 1999). Beam and source shapes are approximated to Gaussians. The source's spatial structures, however, cannot be resolved within the diffraction limit set by the beam angular sizes (4 arc-minutes). A crude estimation of the angular extent occupied by the source with respect to the beam can be obtained by means of the contrast parameter: a ratio between the three corrected antenna temperatures. When the source size is small compared to the beam size, the contrast should be high, and the contrary happens for an extended source.

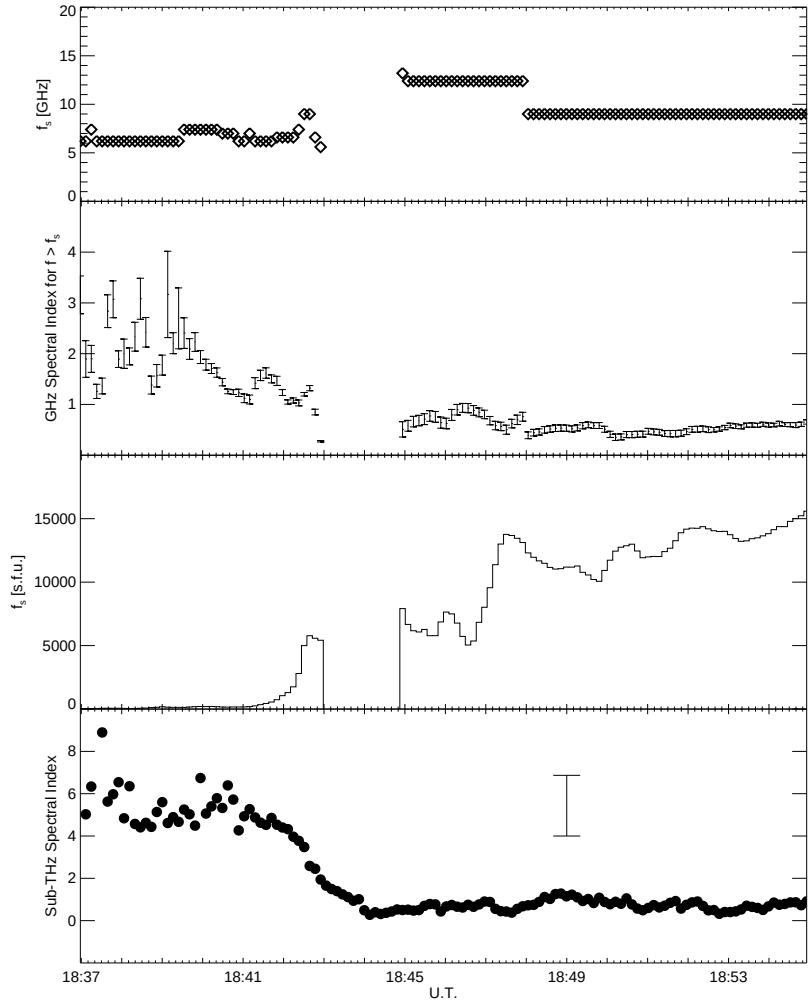

Figure 3. From top to bottom, time variation of: the spectral turnover frequency f_s at microwaves derived from OVSA observations; of the microwave spectral index for $f > f_s$; of the microwave flux at the turnover frequency f_s. Missing data correspond to time intervals where f_s can be higher than the maximum OVSA frequency (18 GHz). Bottom: time variation of the sub-THz spectral index. The bar represents the fixed uncertainty on the 405 GHz flux correction due to atmosphere transmission.

Figure 4 shows the antenna noise temperature time profiles, corrected for atmospheric transmission, for the beams spatially close to the burst location. There is a good temporal agreement during phases **(A)** and **(B)**. 405 GHz time structures at phase **(C)** (beam 5) are not always related to the 212 GHz time structures (beams 2, 3 and 4). This might be attributed to the enhancement of atmosphere transmission variations, substantially larger at 405 GHz. The 212 GHz emission centroid positions shown in Figure 5 have been estimated from 40 ms data and averaged over one second for intervals labeled **(A)**, **(B)** and **(C)** in Figure 1 (top). The sizes and positions for the six SST beams are also shown, with respect to the solar limb at the time of the burst. Since December 2006, the SST pointing model has provided an absolute position accuracy of 10 arc-seconds r.m.s. for all beams (Wallace, 2006). The positions inferred for precursor-like burst (interval **A**) are clearly distinct by about one arc-minute from the positions of the 212 GHz emitting region derived during phases **(B)** and phase **(C)**.

The observed contrasts between the beam outputs at 212 GHz indicate that the source size was at most of the order of the antenna beam size throughout the whole event. Since just one beam is available at 405 GHz no position for emission centers or burst size could be estimated at this frequency. To determine the flux densities, we first compare the corrected antenna temperatures for the three partially overlapping beams to determine the direction for the maximum emission. The maximum antenna temperature is calculated assuming Gaussian shape for the three beams. The calculated fluxes are for sources placed at the direction of maximum emission. They are obtained from the well known relationship for point sources (still valid for sources small or comparable to the half-power beam size),

$$S = \frac{2kT_a}{A_e} \quad , \tag{1}$$

where k is the Boltzmann constant, T_a the antenna temperature and A_e the antenna effective area (0.35 m^2 at 212 GHz and 0.18 m^2 at 405 GHz at the time these measurements were obtained). At 212 GHz the antenna temperature averaged over 8 seconds interval around the burst maximum (at 18 43:51 UT) was $T_a \sim 4900$ K. This corresponds to a flux density of about 3800 s.f.u. at 212 GHz (1 s.f.u = 10^{-22} W m^{-2} Hz^{-1}). The 405 GHz flux densities are similarly calculated by assuming the source has the same position as the 212 GHz source. The mean 405 GHz peak temperature was $T_a \sim 4500$ K corresponding to a flux of 7000 s.f.u. The two temperatures are comparable suggesting emission from an optically-thick source at the two sub-THz frequencies.

The burst fluxes refer to Gaussian-shaped sources with equivalent sizes of the order or smaller than the beam sizes. No estimates can be directly given for actual brightness temperatures of smaller sources that might be scattered and unresolved over the beam extension.

Figure 6 shows emission contours at UV, soft- and hard X-rays taken along time intervals within the three burst phases (see labels at the top of the Figure).

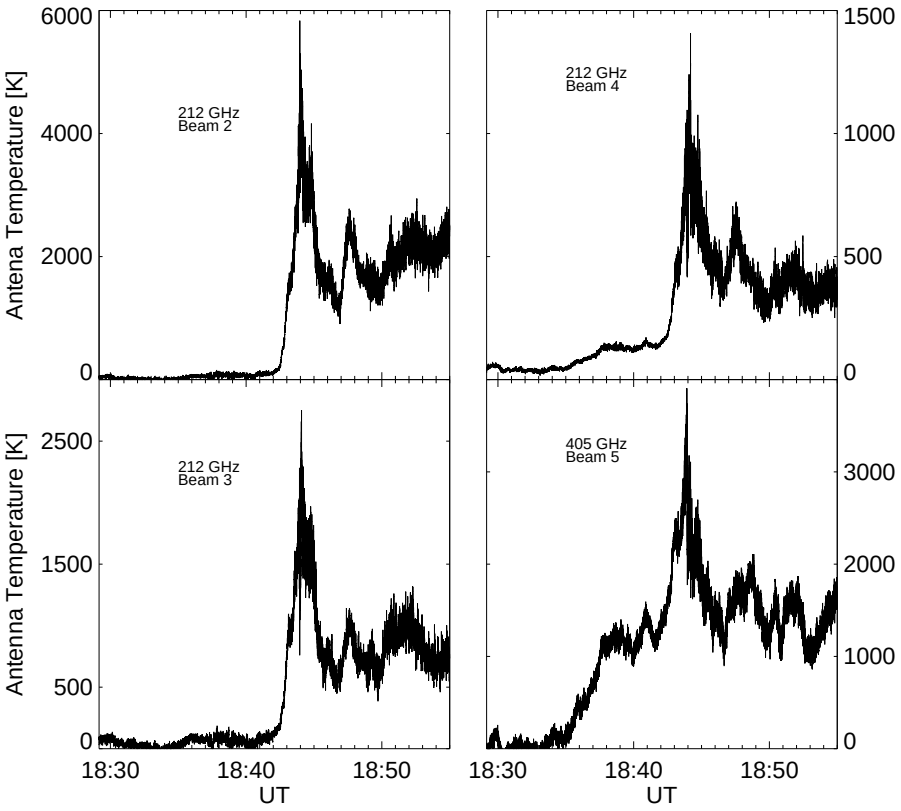

Figure 4. Antenna noise temperatures, corrected for atmosphere transmission, for the SST receivers whose beams are on the burst sources, 5 (405 GHz) 2, 3 and 4 (212 GHz). The beam positions on the solar disc are shown in Figure 5. Note that the temperature scales are different for the different panels. The precursor-like and impulsive time structures are well correlated. The following phase 212 GHz fluctuations are poorly related to the 405 GHz time variations, which might receive considerable influence from atmosphere transmission variations.

The precursor-like phase **(A)** was detectable only at softer RHESSI X-ray energies (> 6 and > 20 keV). The source is located about 20 arc-sec east from the 212 GHz centroid of emission at interval **(A)**. Two small RHESSI hard X-ray source (> 50 keV) appear at intervals **(B)** and **(C)**. The southern hard X-ray source displaces further south by about 20 arc-sec from phase **(B)** to phase **(C)**. The 212 GHz emission centroids at phases **(B)** and **(C)** are displaced in the SE direction by almost 1 arc-min. There is a suggested centroid concentration at phase **(C)**, displaced and close to the general hard X-Ray source position. The background UV TRACE images indicate complex spatial structures. Since the 212 GHz beam angular sizes are larger than the frame angular sizes, they may

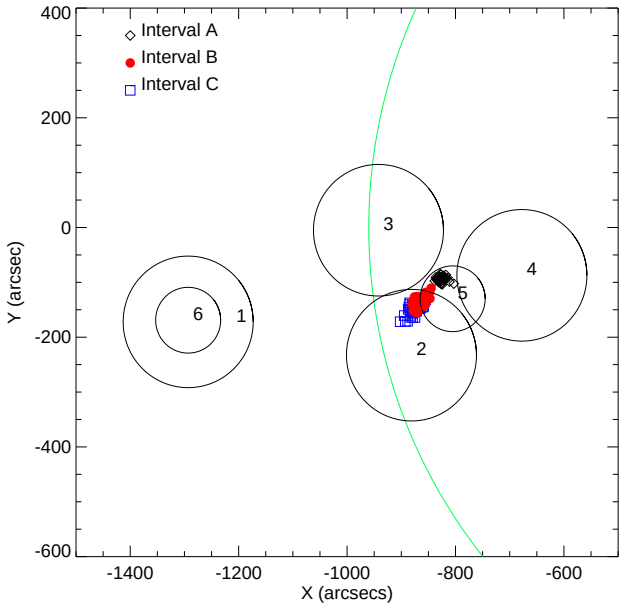

Figure 5. The positions for the 212 GHz burst centroids of emission, averaged every second along the time intervals indicated in the top of Figure 1, for phases **(A)** (precursor), **(B)** (impulsive) and **(C)** (following). The precursor position is clearly displaced by about one arc-minute from the remaining burst phases, which are close by about 30 arc-seconds to each other. The six SST antenna beams are shown with respect to the solar disk at the time of the burst. They are considerably larger than the emitting source centroid displacements. For the precursor-like phase the 212 GHz centroid of emission is closer to beams 3 and 4 producing larger corrected antenna temperatures, shown in Figure 4.

subtend a number of unresolved sub THz sources.

4. Discussion

The December 6, 2006 flare exhibited the THz spectral component throughout the event duration. It is particularly evident since the early phase **(A)**, previous to the impulsive enhancement. The spectrally separated microwaves component was always present, exhibiting a turnover frequency at about 6-7 GHz prior to the impulsive phase **(A)**, when it raised to about 15-13 GHz **(B)**, staying at about 10 GHz during the remaining time.

4.1. Thermal interpretation

From GOES observations we derived the mean emission measure $EM = 10^{50}$ **cm**$^{-3}$ **and temperature** $T = 2.4\ 10^{7}$ **K (calculated after** Garcia**,** 1994 **and** Feldman, Laming, and Doschek**,** 1995**) during the interval**

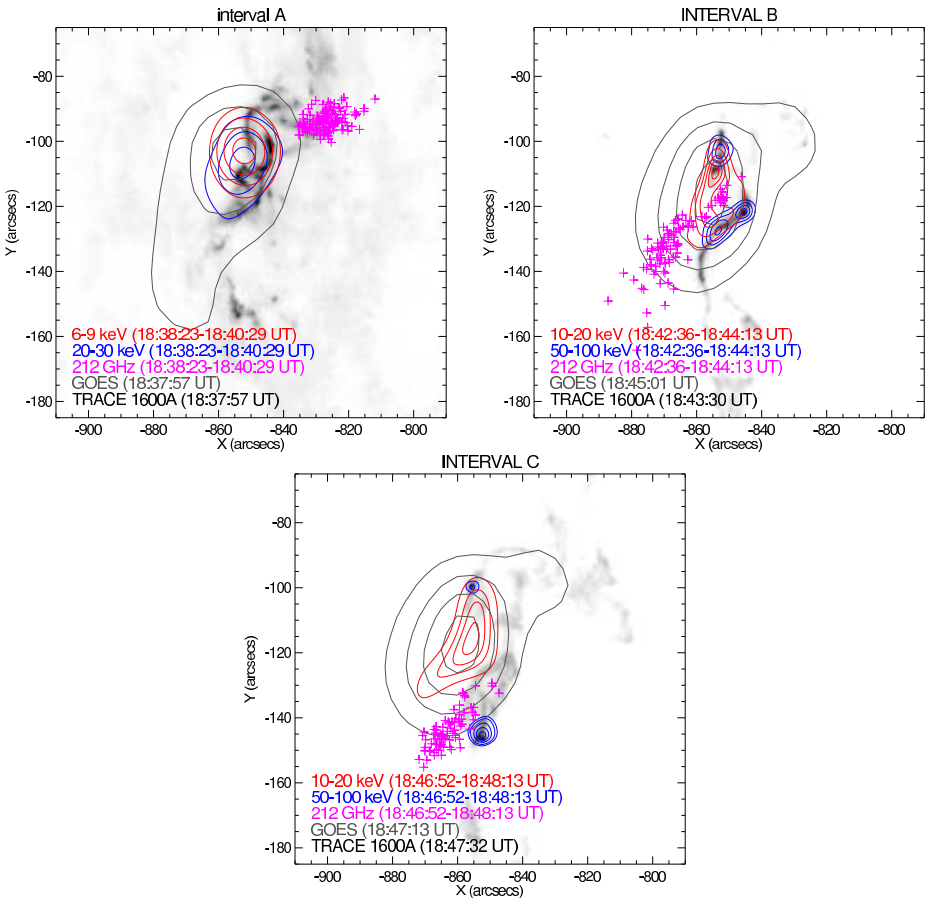

Figure 6. RHESSI hard X-ray (thermal emission in red and non-thermal in blue contours), GOES soft X-ray **(thin black contours)**, and TRACE UV images **background continuum gray-black areas** during phase **(A)**, **(B)**, and **(C)**(see Figure 1). 212 GHz centroid positions (same as in Figure 5) are shown as magenta crosses for comparison.

1843:30 – 1845 UT, which corresponds to the maximum emission at the sub-THz frequencies. Images from the SXI on GOES-12 revealed a soft-X ray flaring size of approximately 1.5 arc min. With these values, the maximum expected free-free emission (e.g. Dulk, 1985**) of a homogeneous source is ∼ 100 s.f.u. with a turnover frequency around 10 GHz. It is orders of magnitude smaller than the observed radio fluxes. Nonetheless, we can investigate the necessary conditions that a thermal source should provide to account for the increase in flux above 200 GHz.**

The optical depth τ_{ff} for free-free emission (e.g. Ohki and Hudson, 1975) is given by

$$\tau_{ff} \simeq 0.19 \frac{N^2 H}{T^{3/2} \nu^2} \quad , \tag{2}$$

where N is the electron density, T the plasma temperature, H is the source lenght in the line of sight and can be considered $H \simeq D_s$ with D_s the source scale size and ν the frequency. We may try to reconcile this brightness to the observed antenna temperatures from the well known approximation:

$$T_a \simeq T_b \frac{\Omega_s}{\Omega_a} \quad , \tag{3}$$

where Ω_s is the source solid angle size and Ω_a the antenna beam solid angle, can be approximately written as:

$$T_a \simeq T_b \left(\frac{D_s}{D_a} \right)^2 \quad , \tag{4}$$

where D_a is the projected size on the Sun of the antenna beam. Equating (4) with (2) we obtain

$$N^2 \simeq 5.26 \; \tau_{ff} \; \frac{T_a^{3/2} \; D_a^3 \; \nu^2}{D_s^4} \quad . \tag{5}$$

For source sizes smaller than about 30 arc-seconds the interpretation in terms of optically thick ($\tau_{ff} > 1$) free-free emission becomes inconsistent with the 212 and 405 GHz measurements because it implies in an emission measure **several orders of magnitude larger than the one obtained**. Thus, like for other events exhibiting the THz component, the thermal interpretation is not consistent with a compact source (Kaufmann *et al.*, 2004; Kaufmann and Raulin, 2006; Silva *et al.*, 2007; Trottet *et al.*, 2008).

4.2. Non-thermal interpretation

If the 212 and 405 GHz sources are small, non-thermal mechanisms by high energy particles (electrons and ions) have to be considered to produce the emissions observed during the December 6, 2006. If a number of plausible source and medium parameters are assumed, **the optically thick gyrosynchrotron emission and the free-free absorption might be taken in consideration to account for the observed flux increase with frequency. Assuming, for example, a burst cylindrical volume with ~ 1 arc-second diameter and ~ 1 arc-second height, on a plasma medium with ambient density of $\sim 10^{12}$ cm^{-3} and a temperature of a few 10^5 K, implies in a moderate τ_{ff}(200 GHz) ~ 2. If the flaring area has a magnetic field $B \sim 2000$ G, and the non-thermal electrons a mean density $\sim 10^{10}$ cm^{-3} for energies**

$E \geq E_\circ = 25$ **keV the self-absorption will also contribute with the attenuation of the microwaves while still producing enough emission at the sub-THz domain.** Of course the two sub-THz frequencies data points for the December 6, 2006 burst are not sufficient to define the complete synchrotron spectrum and the various parameters involved to shape it.

A challenging explanation is needed for the "double spectral" emission, with one microwave component peaking between 6 and 15 GHz and another spectrally independent component peaking somewhere in the THz range. One explanation might conceive independent accelerators at the flaring source, producing different energy electrons nearly simultaneously, emitting at two spectral components. However the observations available are too limited to bring any favorable evidence for this possibility. Another scenario suggested by Wild and Smerd (1972) might be adopted, placing a single accelerator closer to a single polarity footpoint injecting electrons into a magnetic morphology split into two separate loops, one low altitude with stronger field, another weaker field, higher above the solar surface, originating the two synchrotron spectral components. Although this possibility was suggested in the discussion of other bursts of this class (Silva *et al.*, 2007; Trottet *et al.*, 2008; Cristiani *et al.*, 2008), it requires a number of selective free assumptions for the emissions not sufficiently constrained by the existing observations.

Synchrotron emission from high energy positrons was first proposed by Lingenfelter and Ramaty (1967) to account for microwaves. **More recently,** Trottet (2006) **suggested that positrons from charged pions would be an attractive possibility to explain the THz component. Indeed, for one event,** Trottet *et al.*, (2008) **showed that: (i) the 210 GHz impulsive phase emission started simultaneously with the pion production and; (ii) the 210 GHz emitting source coincided with a region of ion interactions, distinct from regions of electron interactions. Such an interpretation cannot be quantitatively studied in the case of the December 6, 2006 flare because the γ-ray emission from this flare was only measured below 17 MeV by RHESSI. This is a too low energy to estimate the relative contributions of pions and electrons to the $>$ 10 MeV gamma-ray continuum (cf** Vilmer *et al.*, , 2003 **and references therein). Nevertheless, it should be noted that, for similar events, the number of positrons needed to explain the sub-THz emission was found much larger than that derived from gamma-ray measurements (**Silva *et al.*, 2007**;** Trottet *et al.*, 2008**). We should note, however, that** there is a theoretical possibility for enhanced positron production by proton-proton interactions by the Drell-Yan process (Szpiegel, Durães, and Steffens, 2007).

Another **suggestion was given** by simulations **of fully relativistic electron beams propagating into high density and high magnetic field medium, generating Langmuir waves producing strong backward emissions with intensities larger at higher sub-THz frequencies as observed** (Sakai *et al.*, 2006). **The same beam, with energies of about 2**

MeV, might also produce the 10-20 GHz microwaves as observed. this possibility was also simulated using proton beams (Sakai and Nagasugi, 2007). **However, these simulations have not taken into account the importance of absorption by the surrounding dense medium**.

These interpretations, however, cannot account well for the "double-peak" spectrum as observed in the microwave-submillimeter range. **One explanation can be given by assuming particle-wave instabilities in beams of ultra-relativistic accelerated electrons, known as "microbunching". The THz spectral component is attributed to incoherent synchrotron radiation (ISR) emitted by ultra-relativistic beams of electrons. The beams are bunched when traversing inhomogeneous magnetic field structures, which are known to be common to sunspots (**Sturrock, 1987**; **Antiochos, 1998**; **Zhang, 2005**). The GHz spectral component arises from the broadband coherent synchrotron radiation (CSR) produced by a wave-particle instability, as a result from the bunching of the high energy accelerated electron beams. The mechanism that produce intense broadband CSR was known for long time (**Nodvick and Saxon, 1954**),but only recently recognized in laboratory accelerators (**Williams, 2002**; **Carr *et al.*, 2002**; **Byrd *et al.*, 2002**). It was shown that this process was possible to happen in solar flares (**Kaufmann and Raulin, 2006**; **Klopf, 2008**). The mechanism is highly efficient. The total power emitted by a bunch is proportional to the total number of electrons in the beam emitting the observed ISR peaking in the THz range, according to the standard interpretation, while the CSR peaking in the GHz range is proportional to the square of the same number times a form factor (**$0 \leq f \leq 1$, Nodvick and Saxon, 1954**). This means that only a small fraction of the accelerated electrons satisfying this condition are needed to account for the observed microwaves**.

The same electron beams producing the ISR may eventually collide into denser regions in the solar atmosphere producing X- and γ-rays by bremsstrahlung. **It has been shown that the ISR spectral contribution to the observed X- and γ-rays might also become significant, although not a necessary condition (**Kaufmann and Raulin, 2006**)**. The number of electrons required to produce the hard X- and γ-rays emissions should be compared to the number of electrons needed to produce the ISR spectrum in the THz range (rather than at microwaves as is usually done). This approach may bring a possible explanation to the electron number discrepancy, also known as the "electron number paradox" (Brown and Melrose, 1977; Kai, 1986).

5. Concluding remarks

The sub-THz emitting region could not be spatially resolved during the December 6, 2006 event. Therefore, a thermal interpretation of the radio emission

above 200 GHz cannot be discarded if we assume a single source whose size is larger than 30 arc-seconds. However, the rather good similarity between hard X-ray and sub-THz time profiles and the fact that hard X-rays are emitted in discrete sources with diameters of the order of 10 arc-seconds, suggest that the sub-THz radiation was produced in several non-thermal sources. If this is the case, the emission, which should peak in the THz region, might be attributed to incoherent synchrotron radiation (ISR) from ultra relativistic electrons or positrons..

A non-thermal interpretation brings questions on the nature of the microwave spectra observed together with the sub-THz emission. Possibilities discussed above suggest that electrons are injected into different magnetic arches of different magnetic field strengths and electronic densities. in order to produce the two separate synchrotron spectral components. The Razin effect might play a role to suppress the optically thin synchrotron emission below 400 GHz.

The microwave emission might be at least partially produced by another mechanism recently recognized in laboratory accelerators. Indeed, intense broadband coherent synchrotron radiation (CSR) in the microwave range may be produced as the result of the bunching of high energy electron beams. These beams also produce the incoherent synchrotron radiation (ISR) in the THz range. The electron beams producing the ISR may eventually collide into denser regions where they may contribute to the X- and γ-ray bremsstrahlung continuum. It should also be noted that additional contribution to hard X-rays and gamma-rays might come from the high frequency part of the ISR spectrum.

Progresses in these researches require measurements in the unexplored THz range which are crucial for the understanding of the relative importance of the mechanisms discussed in this study. New experiments are currently being considered to observe solar flares from ground and space. The most advanced is the DESIR (DEtection of Solar eruptive Infrared Radiation) experiment for the France-China satellite SMESE (Small Explorer for the study of solar eruptions, Vial *et al.*, , 2008).

Acknowledgements Comments by one referee were helpful to improve the paper presentation. The authors acknowledge D.E. Gary for making available the OVSA microwave data and the the support given to SST operations by the Complejo Astronomico El Leoncito engineers A. Marun, P. Pereyra, R. Godoy and G. Fernandez. This research was partially supported by Brazilian agencies FAPESP, CNPq, MackPesquisa, Argentina agency CONICET and France agency CNRS.

References

Akabane, K., Nakajima, H., Ohki, K., Moriyama, F., Miyaji, T.: 1973, *Solar Phys.* **33**, 431. doi:10.1007/BF00152430.

Altyntsev, A.T., Fleishman, G.D., Huang, G.L., Melnikov, V.F.: 2008, *Astrophys. J.* **677**, 1367. doi:10.1086/528841.

Antiochos, S.K.: 1998, *Astrophys. J.* **502**, 181. doi:10.1086/311507.
Bastian, T.S., Fleishman, G.D., Gary, D.E.: 2007, *Astrophys. J.* **666**, 1256. doi:10.1086/520106.
Brown, J.C., Melrose, D.B.: 1977, *Solar Phys.* **52**, 117.
Byrd, J.M., Leemans, W.P., Loftsdottir, A., Marcelis, B., Martin, M.C., McKinney, W.R., Sannibale, F., Scarvie, T., Steier, C.: 2002, *Phys. Rev. Lett.* **89**(22), 224801. doi:10.1103/PhysRevLett.89.224801.
Carr, G.L., Martin, M.C., McKinney, W.R., Jordan, K., Neil, G.R., Williams, G.: 2002, *Nature* **420**, 153. doi:10.1038/nature01175.
Cogdell, J.R.: 1972, *Solar Phys.* **22**, 147. doi:10.1007/BF00145471.
Costa, J.E.R., Correia, E., Kaufmann, P., Magun, A., Herrmann, R.: 1995, *Solar Phys.* **159**, 157.
Cristiani, G., Gimenez de Castro, C.G., Mandrini, C.H., Machado, M.E., de Benedetoo e Silva, I., Kaufmann, P., Rovira, M.G.: 2008, *Solar Phys.*. in press.
Croom, D.L.: 1970, *Solar Phys.* **15**, 414. doi:10.1007/BF00151848.
Croom, D.L.: 1971a, *Solar Phys.* **19**, 152. doi:10.1007/BF00148831.
Croom, D.L.: 1971b, *Solar Phys.* **19**, 171. doi:10.1007/BF00148832.
Dulk, G.A.: 1985, *Ann. Rev. Astron. Astrophys.* **23**, 169.
Feldman, U., Laming, J.M., Doschek, G.A.: 1995, *Astrophys. J.* **451**, 79. doi:10.1086/309695.
Garcia, H.A.: 1994, *Solar Phys.* **154**, 275.
Gary, D.: 2008, In: *Proc. International Ionospheric Effcts Symposium (URSI/ONR/AFSOR)*, 058.
Georges, C.B., Schaal, R., Costa, J., Kaufmann, P., Magun, A.: 1989, In: *SBMO-International Microwave Symposium/Brazil IEEE Catalog N89th0260-0* **447**.
Giménez de Castro, C.G., Raulin, J.P., Makhmutov, V.S., Kaufmann, P., Costa, J.E.R.: 1999, *Astron. Astrophys. Suppl.* **140**, 373.
Kai, K.: 1986, *Solar Phys.* **104**, 235.
Kaufmann, P., Raulin, J.P.: 2006, *Physics of Plasmas* **13**, 701. doi:10.1063/1.2244526.
Kaufmann, P., Correia, E., Costa, J.E.R., Vaz, A.M.Z., Dennis, B.R.: 1985, *Nature* **313**, 380.
Kaufmann, P., Raulin, J.P., de Castro, C.G.G., Levato, H., Gary, D.E., Costa, J.E.R., Marun, A., Pereyra, P., Silva, A.V.R., Correia, E.: 2004, *Astrophys. J.* **603**, 121.
Kaufmann, P., Trottet, G., Giménez de Castro, C., Raulin, J., Gary, D., Fernandez, G., Godoy, R., Levato, H., Marun, A., Pereyra, P.: 2007, In: *American Astronomical Society Meeting Abstracts, American Astronomical Society Meeting Abstracts* **210**, 93.
Klopf, J.M.: 2008, In: *1st SMESE Workshop, 10-12 March 2008, Institut d'Astrophysique de Paris*.
Lingenfelter, R.E., Ramaty, R.: 1967, *Planet. Space Sci.* **15**, 1303.
Nita, G.M., Gary, D.E., Lee, J.: 2004, *Astrophys. J.* **605**, 528. doi:10.1086/382219.
Nodvick, J.S., Saxon, D.S.: 1954, *Phys. Rev.* **96**(1), 180. doi:10.1103/PhysRev.96.180.
Ohki, K., Hudson, H.S.: 1975, *Solar Phys.* **43**, 405.
Ramaty, R., Schwartz, R.A., Enome, S., Nakajima, H.: 1994, *Astrophys. J.* **436**, 941.
Roy, J.R.: 1979, *Solar Phys.* **64**, 143.
Sakai, J.I., Nagasugi, Y.: 2007, *Astron. Astrophys.* **474**, 33. doi:10.1051/0004-6361:20078471.
Sakai, J.I., Nagasugi, Y., Saito, S., Kaufmann, P.: 2006, *Astron. Astrophys.* **457**, 313. doi:10.1051/0004-6361:20065368.
Shimabukuro, F.I.: 1970, *Solar Phys.* **15**, 424.
Silva, A.V.R., Share, G.H., Murphy, R.J., Costa, J.E.R., de Castro, C.G.G., Raulin, J.P., Kaufmann, P.: 2007, *Solar Phys.* **245**, 311. doi:10.1007/s11207-007-9044-0.
Sturrock, P.A.: 1987, *Solar Phys.* **113**, 13.
Szpiegel, S., Durães, F.O., Steffens, F.: 2007, *Braz. J. Phys.* **37**, 52.
Trottet, G.: 2006, In: Fang, C., Schmieder, B., Ding, M. (eds.) *Third French-Chinese Meeting on Solar Physics: Solar Activity: Progress and Prospects, Nanjing University Press*, 82.
Trottet, G., Krucker, S., Lüthi, T., Magun, A.: 2008, *Astrophys. J.* **678**, 509. doi:10.1086/528787.
Vial, J.C., Auchère, F., Chang, J., Fang, C., Gan, W.Q., Klein, K.L., Prado, J.Y., Rouesnel, F., Sémery, A., Trottet, G., Wang, C.: 2008, *Advances in Space Research* **41**, 183. doi:10.1016/j.asr.2007.07.007.
Vilmer, N., MacKinnon, A.L., Trottet, G., Barat, C.: 2003, *Astron. Astrophys.* **412**, 865. doi:10.1051/0004-6361:20031488.
Wallace, P.: 2006, Tpoint technical report tps/06/11/sst. Technical report.

Wild, J.P., Smerd, S.F.: 1972, *Ann. Rev. Astron. Astrophys.* **10**, 159. doi:10.1146/annurev.aa.10.090172.001111.
Williams, G.P.: 2002, *Rev. Sci. Instrum.* **73**, 1461.
Zhang, H.: 2005, In: Dere, K., Wang, J., Yan, Y. (eds.) *Coronal and Stellar Mass Ejections*, *IAU Symposium* **226**, 161.